Oceanologia, 67 (4)/2025, 67406
Polish Academy of Sciences
Institute of Oceanology

https://doi.org/10.5697/GRSC5449

Long-term variability of sound speed conditions in Hornsund fjord, Svalbard, between 2001 and 2019

Pavani Vithana Madugeta Vidanamesthrige*[,1], Natalia Gorska[1], Oskar Głowacki[2]

Abstract
The glacierised Arctic fjords are particularly sensitive to oceanic and atmospheric warming caused by climate shifts; the melting of glaciers and icebergs is one of the major indicators of this sensitivity. The meltwater delivery to the ocean changes the thermohaline structure of the water column, which not only affects water mixing but also controls the sound speed conditions; the latter is crucial for the variability of underwater sound propagation. Finally, changes in sound propagation conditions affect marine animals that rely on sound for their key biological functions, such as communication, navigation, and mating. Here, we investigate the long-term variability of sound speed conditions in the Hornsund fjord, Svalbard, together with its governing factors. We calculated the vertical sound speed profiles using temperature and salinity data collected along the fjord centerline from 2001 to 2019. Spatial and temporal variability in sound speed conditions are observed. We identify two major types of sound channels: (i) near-surface sound channel and (ii) deep sound channel. Potential physical mechanisms that govern the presence and position of these sound channels are discussed, including glacier melting, shelf-fjord water exchange, and atmospheric heat flux. In recent years, the climate-driven transformation of Hornsund has led to the disappearance of deep sound channels due to the intensified inflow of Atlantic Water, and an increased presence and extent of near-surface sound channels resulting from elevated freshwater input from melting glaciers. We suggest that climate warming-induced changes in sound speed conditions in Hornsund are likely to have far-reaching consequences for underwater sound pollution, potentially impacting the well-being of marine animals.

Keywords
Hornsund; Glacier melting; Shelf-fjord water exchange; Underwater sound; Marine mammals

[1]*Institute of Oceanology, Polish Academy of Sciences, Powstańców Warszawy 55, 81-712 Sopot, Poland*
[2]*Institute of Geophysics, Polish Academy of Sciences, Księcia Janusza 64, 01-452 Warszawa, Poland*
***Correspondence**: pavani@iopan.pl (P. V. Madugeta Vidanamesthrige)

Received: 28 October 2024; **revised:** 19 August 2025; **accepted**: 16 September 2025

1. Introduction

Arctic fjords are one of the major hotspots of climate shifts (Dahlke et al., 2020; Gjelten et al., 2016; IPCC, 2021; Wawrzyniak and Osuch, 2020). Warming atmosphere and oceans are causing rapid melting of glaciers, sea-ice, and icebergs (e.g., Błaszczyk et al., 2023; Cook et al., 2019; Holmes et al., 2019; Luckman et al., 2015; Slater and Straneo, 2022). The delivery of freshwater from melting glacier ice and sea-ice disappearance impacts the underwater soundscape of glacierised fjords in two ways. First, the generation of underwater noise due to the activity of noise sources of glacier origin, such as ice melting and glacier calving events (e.g., Deane et al., 2014; Glowacki, 2020; Glowacki et al., 2015; Matsumoto et al., 2014; Pettit et al., 2015; Podolskiy et al., 2022). Moreover, the shipping traffic in the Arctic increases due to the accelerating sea-ice loss (e.g., PAME 2019; PAME 2025; Rodriguez et al., 2024). The analysis of the data presented in the Coastal Data House of Norwegian Coastal Administration confirms the increase in the number of vessels in the fjords of Spitsbergen (Kystdatahuset, 2025). Second, the melting of glacier ice affects the sound speed conditions in the water column (Glowacki et al., 2013, 2016; Vishnu et al., 2020). The latter has important implications for how far different sounds will travel, and therefore influences the sound pollution in fjords, as it was demonstrated for the Arctic region (e.g., Affatati et al., 2022; Duda, 2017; Possenti et al., 2023). Changes in underwater soundscapes can cause behavioral disturbance, hearing damage, and masking of important sounds generated and received by marine animals that influence their well-being by impacting key biological functions: communication, navigation, feeding, and mating behavior (e.g., Duarte et al., 2021; Erbe and Farmer, 2000; Erbe et al.,

2016; Halliday et al., 2017, 2019, 2020; Lyamin et al., 2011; Martin et al., 2022; PAME, 2019). Moreover, the knowledge about the sound propagation conditions and their variability is critical whenever the sound is used for studying environmental phenomena and utilizing underwater acoustic communication systems (e.g., Chitre et al., 2008; Deane, 2019). Therefore, there is a growing importance of understanding the changes in sound speed conditions in glacierised Arctic fjords.

The sound speed in seawater is determined by temperature, salinity and pressure (Urick, 1979). Changes in water temperature contribute the most in terms of sound speed variability. However, the impact of salinity becomes important in regions that are characterised by substantial salinity changes (e.g., Glowacki et al., 2013; Jensen et al., 2011). One notable example is the fjords of West Spitsbergen, where remarkable spatial and temporal variability in the thermohaline structure has been observed during recent decades due to both temperature and salinity changes (e.g., Promińska et al., 2017, 2018; Skogseth et al., 2020; Tverberg et al., 2019). Different climate-driven environmental factors control the variability of the thermohaline structure in the West Spitsbergen fjords. Some of them are: the freshwater delivery from melting glaciers, warm water advection to the fjord, and variations of air temperature and precipitation (Arntsen et al., 2019; Błaszczyk et al., 2019; Promińska et al., 2018; Skogseth et al., 2020; Strzelewicz et al., 2022; Tverberg et al., 2019).

Local minima in the temperature- and salinity-controlled sound speed profiles indicate positions of underwater sound channels, which play an important role in changing sound propagation conditions (Medwin and Clay, 1998; Urick, 1979). Sound energy is focused in the channel, because acoustic waves are refracted towards the region of lower sound speed. Sound waves trapped inside the channel can propagate for long distances with minimal energy loss due to the limited interactions with the sea surface and bottom. The sound channel axis is at the depth of the local sound speed minimum. Underwater sound channels are common features in the global ocean; they can be formed near the surface or deeper in the water column and near the seabed, depending on the vertical distribution of water temperature and salinity. For example, the sound speed minimum at the larger depths (about 800–1000 m) at mid-latitudes creates a deep ocean sound channel called Sound Fixing and Ranging (SOFAR) (Munk et al., 1995). In deep oceans, the temperature decreases with increasing depth and tends to decrease the sound speed. From a certain depth onward, temperature becomes constant (about depths below 800–1000 m). Then, the sound speed increases with depth due to the hydrostatic pressure increase. These phenomena cause the sound waves directed upwards from the channel axis to refract downward. On the other hand, it causes sound waves directed downwards from the channel's axis to refract upward.

In the eastern Arctic Ocean, the sound speed minimum is usually observed near the sea surface (Jensen et al., 2011; Kutschale, 1969; Worcester et al., 2020). In such a case, the sea surface is typically covered with ice, and a layer of cold and less saline water is just under it. This thermohaline structure creates the near-surface sound channel. In the western Arctic, the sound channels are different from those in the eastern Arctic because of the presence of the Pacific-origin waters (Baggeroer and Collis, 2022; Ballard et al., 2020; Duda, 2017; Duda et al., 2021; Kucukosmanoglu et al., 2023; Worcester et al., 2020, 2022). The sound channel, known as the Beaufort duct, forms at the water layers occupied by the cold Pacific Winter Water (PWW). The Atlantic and Pacific Summer Waters (AW and PSW), located respectively below and above the PWW layer, keep the Beaufort duct away from the sea surface and bottom.

In Hornsund, one of the West Spitsbergen fjords, measurements of water temperature and salinity made in glacial bays during the summer months demonstrated that the minimum sound speed near the surface was accompanied by the cold, fresh meltwater discharged from marine-terminating glaciers (Glowacki et al., 2013, 2016; Vishnu et al., 2020). Accordingly, Glowacki et al. (2013, 2016) described the near-surface sound channel created at the close vicinity of one of the marine-terminating glaciers by the presence of glacially modified water in the surface layer. Vishnu et al. (2020) studied the sound speed profiles and the corresponding sound propagation conditions in a few glacial bays of Hornsund fjord. Overall, previous studies have demonstrated that glacial bays are characterised by the common feature of the near-surface sound channel.

The long-term climate-driven variability of underwater sound channels in the Arctic Ocean and its potential future development has been reported in numerous studies (e.g., Affatati et al., 2022; Duda, 2017; Lynch et al., 2018; Possenti et al., 2023; Worcester et al., 2020). Changes in the extent of sea-ice cover and modification of the thermohaline structure of the water column are considered as key mechanisms that influence sound speed conditions and the formation of sound channels (Lynch et al., 2018; Storheim et al., 2022; Worcester et al., 2020). In the case of near-surface sound channels, the sound waves can interact with sea ice and glacier ice through scattering and reflection, as well as the energy conversion from the incident sound wave in water into compressional and shear waves within the ice (McCammon and McDaniel, 1985; Meyer et al., 2019; Worcester et al., 2020). As a consequence, changes in the distribution, morphology and extent of ice on the sea surface can dramatically change sound propagation conditions in polar regions (e.g., Alexander et al., 2016; Ballard, 2019; Diachok, 1976; Lynch et al., 2018; Zeh et al., 2022).

In the case of changes in thermohaline structure, the PSW and AW – located respectively above and below the cold and saline PWW – have warmed and thickened in re-

cent years. It caused the Beaufort duct to become "stronger", i.e. the difference between the maximum sound speed within PSW and AW and the minimum sound speed within PWW has increased (Ballard et al., 2020; Duda et al., 2021; Lynch et al., 2018; Worcester et al., 2020, 2022).

To the best of our knowledge, the long-term variability of sound speed conditions in Hornsund has not been studied. Moreover, the previous studies of sound speed conditions in the Hornsund fjord mostly concerned individual glacial bays and not the entire fjord system (Glowacki et al., 2013, 2016); Vishnu et al., 2020). The impact of fjord-shelf water exchange and other environmental factors on the sound speed profiles in Hornsund was not analysed. This paper sets out to address these research gaps by covering the year-to-year variability of sound speed profiles in the Hornsund fjord during the last two decades. Particular emphasis is placed on the location of sound channels in the water column and the corresponding physical mechanisms that affect the thermohaline structure of the fjord.

The paper is organised as follows. The description of the study area is in Section 2. The next section presents the dataset and methods applied in this study (Section 3). This is followed by the results and discussion of the vertical and horizontal variability of sound speed conditions along the fjord axis: from its mouth (fjord's Outer Part: adopted from Promińska et al., 2018) through its main part to the most eastern part – Brepollen (Section 4). The main types and locations of sound channels, as well as physical mechanisms that control their formation, are also considered in this part. Major outcomes and future perspectives are discussed in Section 5. Concluding remarks are provided in the last section.

2. Study area

Hornsund is located between 76°56'–76°94'N and 15°45' –15°78'E in the southernmost part of the West Spitsbergen and is oriented from East to West (Figure 1a). The fjord is approximately 35 km long and 2–12 km wide (Moskalik et al., 2013; Promińska et al., 2017).

For data analysis, Hornsund was divided into three parts: Outer Part, Main Basin and Brepollen (Figure 1b). The borders separating these parts were adopted from Promińska et al. (2018). The Outer Part extends outside from the Hornsund's mouth, which is marked by the line connecting the capes of Worcesterpynten on the northern coast and Palffyodden on the southern coast (see yellow dashed line in Figure 1b). The Hornsund's mouth is flat and relatively shallow, with a depth of about 150 m (Marsz and Styszyńska, 2013; Promińska et al., 2017). The fjord mouth topography may influence the shelf-fjord water exchange (Promińska et al., 2018; Strzelewicz et al., 2022).

The Main Basin is the middle part of the Hornsund fjord. The maximum depth of around 240 m is found in this part of the fjord (Moskalik et al., 2013). Brepollen is the innermost part of the fjord, which is separated from the Main Basin by a sill with a depth of about 50 m (see blue dashed line in Figure 1b). The maximum depth of Brepollen is around 140 m (Moskalik et al., 2013). Brepollen is a highly glaciated region (Figure 1b). The water exchange between the Main Basin and Brepollen is limited only to the upper layers (Jakacki et al., 2017; Promińska et al., 2018).

The West Spitsbergen Shelf is supplied with different water masses delivered by two currents: the West Spitsbergen Current (WSC) and the Spitsbergen Polar Current (SPC) (see Figure 1a; Nilsen et al., 2016). The WSC brings warm (> 3°C) and saline (>34.9) Atlantic Water into the Arctic Ocean along the western coast of Svalbard (Hopkins, 1991; Nilsen et al., 2008). In contrast to the WSC, the SPC is typically limited to the Svalbard continental shelf and often carries a mixture of drift ice from the Barents Sea and relatively less saline (34–34.5) and cold (−1.5–2°C) Arctic Water (Nilsen et al., 2016; Promińska et al., 2018). However, these two water masses – of Arctic origin and of Atlantic origin – can mix at the West Spitsbergen Shelf area. The Transformed Atlantic Water is defined as a water mass mixture with a temperature above 1°C and salinity between 34.7 and 34.9 (Nilsen et al., 2008). The higher degree of Arctic Water occupation in the shelf close to the Hornsund fjord can potentially cool the fjord's local water masses and limit the warm water inflow (Strzelewicz et al., 2022). In contrast, more Atlantic Water on the shelf connected to the fjord facilitates the warm water input to the fjord (Strzelewicz et al., 2022). As a result, the interplay between the WSC and SPC impacts the thermohaline structure of the Hornsund fjord (e.g., Promińska et al., 2018; Strzelewicz et al., 2022).

The WSC is one of the most important factors shaping weather conditions in the Arctic region, including Hornsund (e.g., Walczowski and Piechura, 2011). The air temperature has been increasing over recent decades in Hornsund and across the entire Svalbard (Dahlke et al., 2020; Wawrzyniak and Osuch, 2020). In the period 1979–2018, the positive linear trend of 1.14°C per decade in the mean annual air temperature has been observed in Hornsund (Wawrzyniak and Osuch, 2020). The average warmest month of the same period was July with a mean air temperature of 4.6°C; the highest recorded mean air temperature was 6.3°C in 2016 (Figure S1 in Supplementary materials) (Wawrzyniak and Osuch, 2020).

About 67% of the Hornsund drainage basin area is covered by glaciers, from which fourteen tidewater glaciers constitute most of the glacierised area (Błaszczyk et al., 2013). The average retreat rate of tidewater glaciers in Hornsund was 70 m yr^{-1} between 2001 and 2010 (Błaszczyk et al., 2013). However, due to the recent climate-driven increase of glacial retreat, the average retreat rate reached 100 m yr^{-1} during 1992–2018 (Błaszczyk et al., 2023). Tidewater glaciers are major sources of freshwater; about 64% of freshwater input to Hornsund is due to the runoff of meltwater and frontal ablation (i.e., submarine

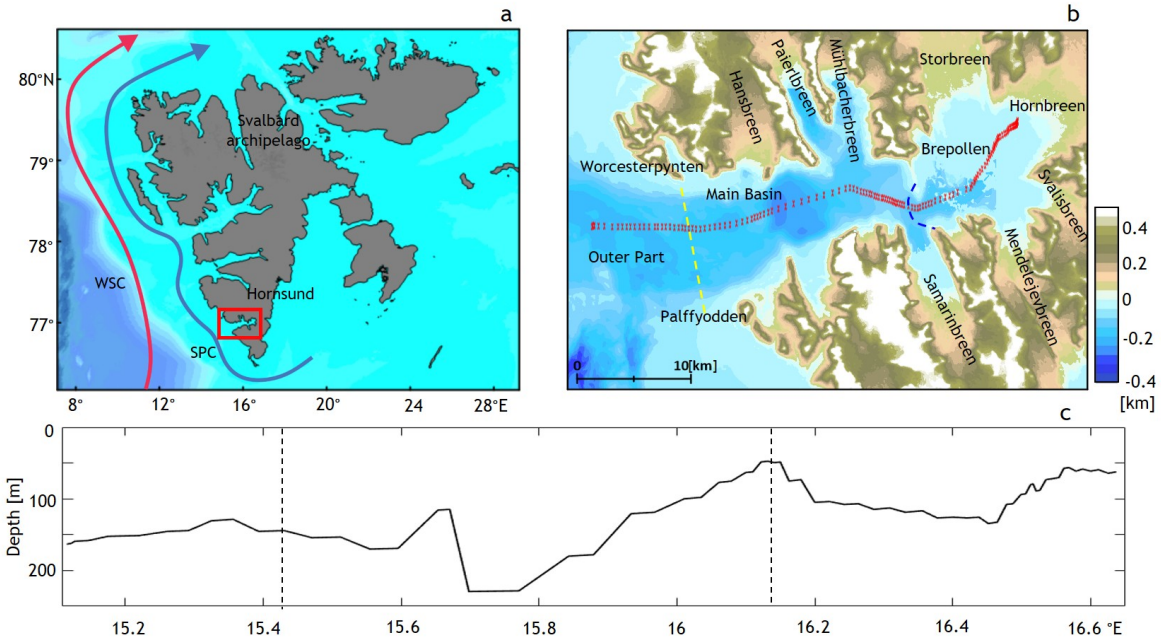

Figure 1. The study area. (a) Svalbard archipelago, the location of Hornsund fjord (red box), and a scheme of the main current systems adopted after Nilsen et al. (2016) (West Spitsbergen Current (WSC-red line) and Spitsbergen Polar Current (SPC-blue line)). (b) the fjord's Outer Part, Main Basin and Brepollen adopted after Promińska et al. (2018). The yellow dashed line separates the Outer Part and the Main Basin. The blue dashed line separates the Main Basin and Brepollen. The positions of the CTD stations in Hornsund are marked with red crosses. (c) Bathymetry along the CTD transect. The black dashed vertical lines indicate boundaries between the Outer Part, Main Basin, and Brepollen.

melting and iceberg calving combined) (Błaszczyk et al., 2019). The freshwater influx has a profound impact on the thermohaline structure of the water column of Hornsund (e.g., Promińska et al., 2018).

In glacierised fjords, the near-surface layer of the water column constitutes glacially modified water, which is a mixture of meltwater and ambient water, and can be as thick as 200 m (Chauché et al., 2014; Straneo et al., 2011). In Hornsund, a thin surface layer of glacially modified water reaching down to 10–15 m below the sea surface and creating a sound channel was revealed at the glacial bays (Glowacki et al., 2016). The sound speed inside this layer typically ranges from 1440 to 1450 m s^{-1}.

3. Material and methods

3.1 CTD data

The analysis presented in this study is based on the temperature, conductivity and pressure data collected by the Institute of Oceanology of the Polish Academy of Sciences during the summer cruises of the r/v *Oceania* in late July or early August from 2001 to 2019. The data were collected using a CTD towed profiling system equipped with the Idronaut 316 probe in the years 2001–2003 and 2006, while the SBE49 probe has been used for other years (Promińska et al., 2018). The locations of CTD stations and the number of CTD vertical profiles varied slightly between the years, though the CTD sections generally followed the same transect (Figure 1b). The instruments were calibrated prior to each cruise (Promińska et al., 2018). The Idronaut 316 was accurate to 0.003°C for temperature and 0.0003 S m^{-1} for conductivity. The SBE 49 probe was accurate to 0.002°C and 0.0003 S m^{-1}, respectively, for temperature and conductivity. The collected data were processed with the SBE Data Processing Software using standard steps and vertically averaged every 1 bar (Promińska et al., 2018). Please note that salinity was calculated from conductivity data using standard procedures. There were no data for the years 2004 and 2005 due to the severe ice conditions and bad data quality, respectively.

3.2 Sound speed calculation and analysis

The sound speed was calculated using the standard Chen and Millero (1977) formula adopted by UNESCO. The formula is as follows:

$$c(S,T,P) = C_w(T,P) + A(T,P)S + \\ + B(T,P)S^{3/2} + D(T,P)S^2, \quad (1)$$

where c is sound speed (m s^{-1}), T is temperature (°C), S is salinity (psu) and P is hydrostatic pressure (Pa). Here, C_w, A, B, and D are functions of the temperature and pressure.

The vertical sound speed profiles were averaged along the transects, separately for each fjord's part. Moreover,

for each depth level, the standard deviation (SD) of the spaced-averaged sound speed along each fjord's part was calculated to analyse the horizontal variability of sound speed across each part separately. Additionally, the min-max normalization was applied to the spaced-averaged vertical sound speed profiles to identify the position of the sound channel axis. It should also be noted that Hornsund's bathymetry is irregular (see Figure 1c), and so there were some stations at which data for depths between 100 and 240 m were not available. At these stations, the average sound speed was calculated only for the available data. All the sound speed calculations, analyses and visualizations were done using the MATLAB software.

4. Results and discussion

4.1 Sound speed conditions in Hornsund fjord during the last two decades: an overview

Figure 2a–c show the vertical profiles of sound speed, averaged along the Hornsund transect separately for the Outer Part, Main Basin and Brepollen, respectively, for the period from 2001 to 2019. Figure 2d–f demonstrate the depth-dependence of the associated SD describing the horizontal variability of the sound speed at different depths. Accordingly, the following sub-subsections give an overview of (i) the inter-annual variability of the space-averaged sound speed (4.1.1) and (ii) horizontal variability of sound speed (4.1.2).

4.1.1 Inter-annual variability of the space-averaged sound speed profiles

Figure 2a shows that in the Outer Part, in most years the space-averaged sound speed was higher than 1460 m s^{-1} in the entire water column (see, e.g., 2006, 2014, 2016 and 2017), while in the Main Basin the values were slightly lower (< 1460 m s^{-1}). In Brepollen, at about 60 m depth, there is a clear transition between two water layers: (i) the upper layer extending up to 10–50 m with sound speed usually higher than about 1455 m s^{-1} and (ii) the bottom layer with sound speed lower than or equal to 1450 m s^{-1} (Figure 2c). Moreover, a narrow region with a sound speed between about 1450 and 1457 m s^{-1} is observed near the sea surface. This sound speed structure in Brepollen is more stable over the years compared to the observed structures in Outer Part and Main Basin (Figure 2a–c).

Furthermore, an exceptional situation was observed in the years 2010–2011 for all three parts of Hornsund. In this period, the sound speed was less than 1455 m s^{-1} in most parts of the water column. The thermohaline structures responsible for this anomaly are discussed below in sub-subsection 4.2.2. Additionally, there were generally lower values of sound speed in 2001–2009 compared to 2012–2019.

We compared how strong the variation of the spaced-averaged sound speed is over depth in different years. In the Outer Part, sound speed exhibited minimal vertical variation in most years. The difference between maximum and minimum averaged values remained below 8 m s^{-1} for more than half (59% or 10 years) of the 17-year study pe-

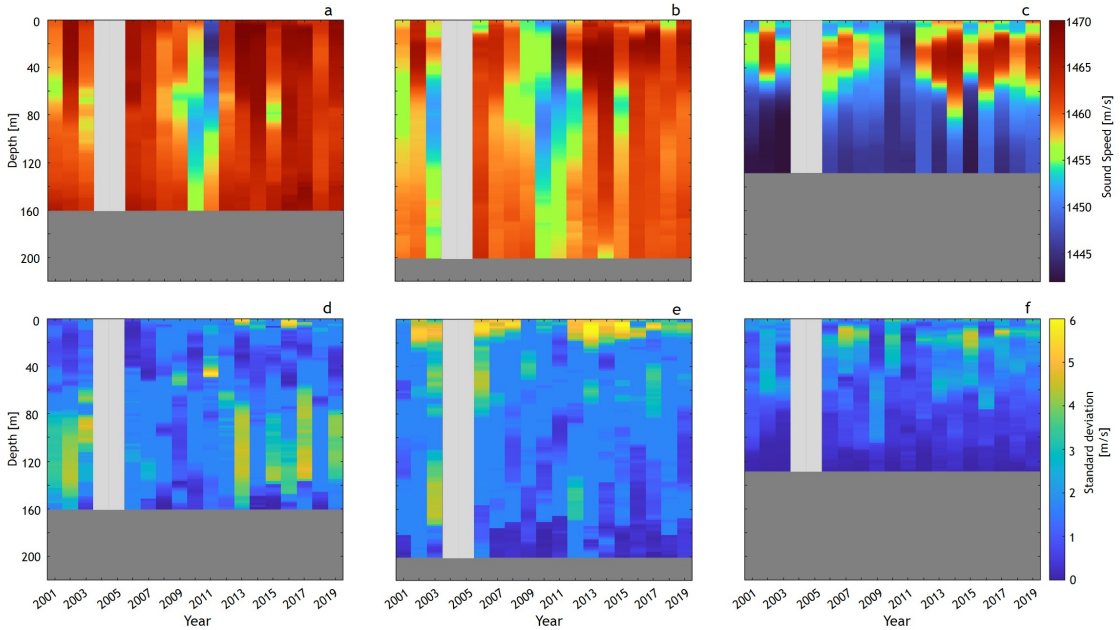

Figure 2. Inter-annual variability of space-averaged vertical sound speed profiles (top row) and the corresponding standard deviations of sound speed (bottom row) computed separately for the Outer Part (a and d), Main Basin (b and e) and Brepollen (c and f). There are no data for 2004 and 2005, as indicated by light grey columns.

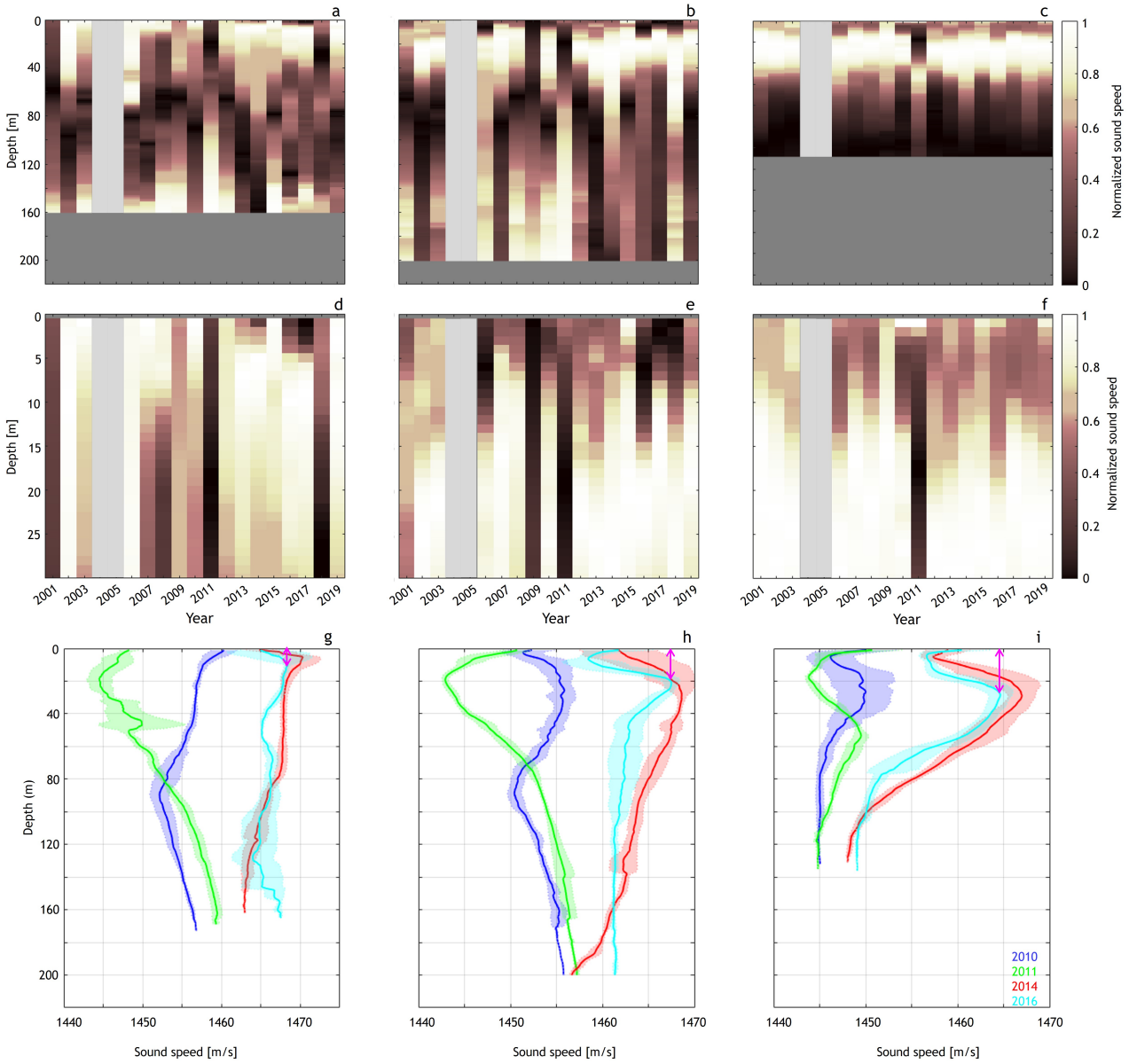

Figure 3. Inter-annual variability of the vertical profiles of normalised space-averaged sound speed for the entire water column (first row) and zoomed view of the top 30 m of the water column (second row) in the Outer Part (a and d), Main Basin (b and e) and Brepollen (c and f). Third row: vertical profiles of space-averaged sound speed in the Outer Part (g), Main Basin (h) and Brepollen (i) in 2010 (dark blue), 2011 (green), 2014 (red) and 2016 (light blue) with corresponding SD (shaded area). Pink double-headed arrows indicate the vertical distance between the sea surface and the shallowest local sound speed maximum in the light blue curve corresponding to the year 2016. There are no data for 2004 and 2005, as indicated by light grey columns in plots a–f.

riod (Figure 2a). In comparison, in the Main Basin and Brepollen, the same difference between maximum and minimum averaged values was observed for shorter periods: 47% (8 years) (Figure 2b) and 12%, (2 years) (Figure 2c) of the entire period, respectively.

4.1.2 Horizontal variability of sound speed profiles

This sub-subsection considers the horizontal variability of the sound speed at each depth along each part of the fjord, quantified as SD (Figure 2d–f). In the Main Basin and Brepollen, the standard deviation was usually below 1 m s^{-1} near the sea bottom (Figure 2e and f, respectively); it demonstrates a uniform horizontal distribution of sound speed. In the Main Basin, the highest SD (> 3 m s^{-1}) was observed in near-surface depths (see e.g., 2006, 2013 and 2015 in Figure 2e); in Brepollen, maximum standard deviations were observed in the middle-upper layer (around

10–60 m) in years 2007, 2015 and 2017, for example (Figure 2f). The highest standard deviations in the Outer Part were often observed for the middle-lower layer (80–140 m depth) (see, e.g., 2002, 2013 and 2017 in Figure 2d). In some years, the horizontal variability of the sound speed in the Outer Part and Main Basin deviates from the patterns presented above. For example, the standard deviation was less than 2 m s^{-1} for the middle-lower layer of the Outer Part in the year 2009 (see Figure 2d). Furthermore, a similar deviation from the general pattern is evident in the Main Basin in years 2001, 2009 and 2011 for near-surface depths (Figure 2e). Deviations are also noticeable in Brepollen (Figure 2f). This analysis demonstrates that the horizontal variability of the sound speed varies between different parts of the Hornsund fjord.

4.2 Underwater sound channels in Hornsund

4.2.1 Positioning of sound channels in the water column

This subsection considers the positioning of sound channels, which depends on the presence and location of sound speed minima in the water column. Figure 3a–f show the vertical profiles of min–max normalised space-averaged sound speed of each fjord's part for: (i) the entire water column (plots a–c) and (ii) a zoomed view of the top 30 m of the water column (plots d–f). After this normalization, the smallest and largest sound speeds are turned respectively to 0 and 1. However, in the presence of two (or more) sound channels at different depths simultaneously, the local minima of normalised sound speed at the sound channel axis could be higher than zero. Accordingly, the dark and light colors indicate lower sound speed and higher sound speed, respectively, in Figure 3a–f. We can identify the presence of sound channels when the dark-coloured region is bounded by light color from the top and bottom or only from the bottom (in some cases). As it was mentioned in the Material and Methods section, the bathymetry of Hornsund is irregular (see Figure 1c); therefore, for each CTD station the number of measurements considered for analysis was depth-dependent. For example, the CTD casts reached 100 m along the entire Main Basin, whereas sampling at 200 m was only possible in a few locations. For this reason, the number of stations for the larger depths could be less than the number of stations in shallower depths. Due to the small number of stations, we did not consider the local minima of normalised sound speed deeper than about 100 m in the discussion. However, we calculated the normalised sound speed for the entire water column. The third row of Figure 3(g–i) shows the line plots of vertical profiles of space-averaged sound speed with corresponding SD (shaded area) for selected years in each fjord's part.

In the Outer Part, the local minima of normalised sound speed were typically observed in the middle of the water column (see, e.g., 2009–2010, 2012 and 2015 in Figure 3a). The position of local minima of normalised sound speed far below the sea surface – as in this case (usually below 60 m) – indicates the presence of a deep sound channel. The 2D spatial distribution of sound speed for individual years in the entire fjord has been analysed. The results of the entire analysis are not presented here. The 2D plots across the regions confirmed that for each year and for each part of the fjord, the presence of a minimum in the normalised averaged sound speed corresponded to the spatially continuous sound channel in this part. For example, the presence of channels in Outer Part and Main Basin in 2010, indicated in Figure 3a–b, is supported further by the Figure 4c, which shows the sound speed distribution along the Outer Part and Main Basin in 2010. The dark blue line in Figure 3g confirms the presence of the deep channel in 2010. It should be borne in mind, however, that in several years deep channels did not develop or their presence is not clear in plots (see, e.g., 2011, 2014 and 2016 in Figure 3g). Figure 3d, in turn, clearly shows the presence of near-surface channels with minima of normalised sound speed just at the surface in 2013, 2014, 2016 and 2017.

In some years in the Main Basin, the local minima of normalised sound speed were observed simultaneously in two regions: (i) in the top 15 m and (ii) in the middle of the water column at around 60–80 m (see, e.g., 2001, 2010, 2012 and 2019 in Figure 3b and e). The locations of local minima of normalised sound speed in the upper layer and middle layer of the water column indicate the presence of near-surface and deep sound channels, respectively. In some years, only near-surface sound channels were clearly observed; some examples are 2006, 2016 and 2017 (Figure 3b,e, and red and light blue curves in plot h).

In Brepollen, the local minima of normalised sound speed in almost all years are located simultaneously in two regions: (i) in the top 10 m of the water column and (ii) between about 60 m and the sea bottom (Figure 3c and f). These upper and bottom layers with the local minima of normalised sound speed indicate the presence of near-surface and near-bottom sound channels, respectively (Figure 3c and f). These two types of channels are also clearly visible in Figure 3i.

Notably, a unique pattern of local minima of normalised sound speed in each part of the fjord occurred in 2011, i.e. the depth of the sound channel axis was constantly between 10 and 30 m along the entire fjord transect (Figure 3a-c). This demonstrates the existence of a long, near-surface sound channel, which is clearly observed in all parts of Hornsund (see also green curves in Figure 3g–i). In other years, the near-surface sound channel was more and more pronounced when moving from the Outer Part towards the inner parts of the Hornsund fjord. It was indicated by the vertical distance between the sea surface and the shallowest local sound speed maximum, which progressively increased toward Brepollen (see, e.g., pink

double-headed arrows in the light blue curve for 2016 in Figure 3g–i).

In Brepollen, the near-surface sound channel was observed during the entire study period. Overall, the interannual variability in the presence and position of sound channels in the Outer Part and Main Basin was higher compared to Brepollen over the period 2001–2019. The analysis has not revealed any clear trends.

4.2.2 Different sound channels: governing factors

In the previous sub-subsection, we discussed the main types of sound channels in Hornsund and their positioning in the water column. Here, we address the physical mechanisms that create those sound channels. For this purpose, it is necessary to discuss different scenarios of thermohaline structure in the Hornsund fjord. Therefore, we identified specific water masses present within and outside sound channels according to the corresponding temperature and salinity ranges criteria adopted by Nilsen et al. (2008).

Deep sound channel

Figure 4 shows two different scenarios of the thermohaline structure developed in the Outer Part and Main basin: one with the presence (left) and one with the lack (right) of the deep sound channel.

In 2010, the deep sound channel was developed in the middle of the water column (see Figure 4c and line plots in Figure 4g). The middle water layer with a temperature range of 0–1°C and a salinity range of 34–34.5, as well as warmer (> 1°C) water masses above and below this layer, controlled the channel presence (Figure 4a–b). The middle water layer contained the Local Water.

In 2014, the deep sound channel was not developed (Figure 4f and h). The water temperature and salinity varied respectively from 5°C and 34 near the surface to 3°C and 35 at depths 100–120 m (Figure 4d–e). This thermohaline structure has prevented the creation of the deep sound channel due to the lack of clear sound speed minima. The water column mostly contained warm water masses: Atlantic Water and Transformed Atlantic Water.

The thermohaline structure of the Outer Part can be directly influenced by two major currents: WSC and SPC (Figure 1a); this is due to its direct connection with the West Spitsbergen Shelf (Promińska et al., 2018; Strzelewicz et al., 2022). Moreover, the Main Basin can interact with the shelf water via the Outer Part (Promińska et al., 2018). Strzelewicz et al. (2022) observed a significant reduction in Atlantic Water advection in some years, especially during 2010, leading to the persistence of Local Water in those parts, which in turn favoured the development of a deep sound channel in that particular year (see Figure 4c and g). Moreover, Promińska et al. (2018) stated the absence of Atlantic Water in the Outer Part in the years 2001, 2003, 2012 and 2015. Our analysis demonstrated that deep sound channels are well-developed in such years (i.e., similar to 2010) (see Figure 3a and b).

Strzelewicz et al. (2022) also mentioned that in some years the WSC is shifted towards the shelf connected with Hornsund, resulting in the dominant residence of Atlantic Water on the shelf. Promińska et al. (2018) have observed an enhanced advection of Atlantic Water into the entire water column of the Outer Part and Main Basin of Hornsund in 2014; as a result, both the Atlantic Water and Transformed Atlantic Water were present in these parts of the fjord. It is in line with the absence of a deep sound channel in 2014, reported here (Figure 4f and h). Furthermore, similar to 2014, Strzelewicz et al. (2022) mentioned the dominant presence of Atlantic Water in the West Spitsbergen Shelf connected with Hornsund in 2017. In certain years, such as 2006 and 2013, Promińska et al. (2018) observed a high content of Atlantic-origin waters in the deep layers of the Outer Part and Main Basin. The above analysis has shown that the dominance of the Atlantic origin water can halt the development of deep sound channels. Summarising, the intensity of shelf-fjord water exchange apparently controls the formation of deep sound channels in the Hornsund fjord.

Near-surface sound channels

Figure 5 illustrates different scenarios of the thermohaline structure developed in Brepollen that led to the creation of near-surface sound channels in 2010 and 2014.

In 2010, the near-surface sound channel was more prominent in the western part of Brepollen compared to its eastern part (pink rectangle in Figure 5c and line plots in Figure 5g). The surface water layer with the temperature lower than 1°C and salinity below 33.3, as well as the warmer (>1°C) and more saline (>33.3) layer below, were responsible for the channel presence (Figures 5a–b). According to the classification described by Nilsen et al. (2008), the Local Water filled the channel region.

In contrast to 2010, in 2014 the near-surface sound channel was developed along the entire Brepollen, becoming wider towards its inner end (see pink rectangle in Figure 5f and line plots in Figure 5h). The surface layer water with the temperature in the range of 2.5–3°C and salinity below 34, as well as more saline (>34) and warmer (> 4°C) water below this layer, controlled the formation of the near-surface sound channel (Figure 5d–e). The surface and sub-surface layers contained Surface Water and warm Intermediate Water, respectively. In addition, there was a very thin layer of warm (> 3°C) Surface Water at the top of the surface layer (Figure 5d).

To understand the factors responsible for the development of near-surface sound channels, it is important to note that Brepollen is a highly glaciated bay (see Figure 1b). During the summer, the thermohaline structure of the glacial bays can be directly influenced by the inflow of freshwater from glacier melting (runoff of meltwater and frontal ablation of tidewater glaciers) (Błaszczyk et al., 2019). The meltwater forms a low salinity and cold surface

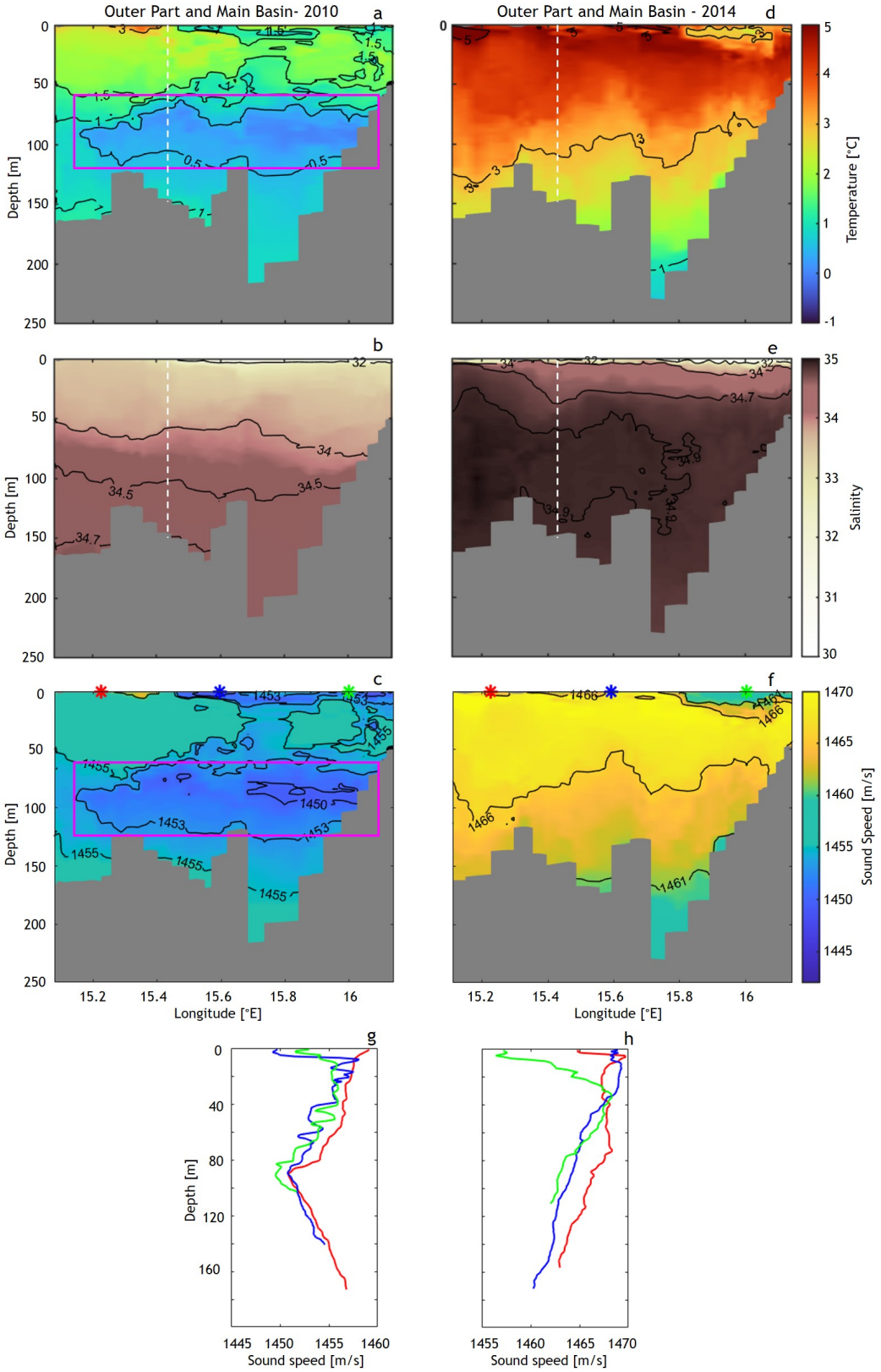

Figure 4. Distribution of water temperature (a and d), salinity (b and e) and sound speed (c and f) in the Outer Part and Main Basin of Hornsund in 2010 (left panel) and 2014 (right panel). The white dashed line indicates the boundary between the Outer Part (left) and the Main Basin (right). Pink rectangles in plots a and c indicate the middle water layer and the location of the deep sound channel, respectively. Sound speed profiles at three selected locations (g and h), marked by red (station in the Outer Part), dark blue (station near the middle of the Main Basin) and green (station near Brepollen) stars in plots c and f. The colors of profiles in plots g and h correspond to the colors used to indicate the stations.

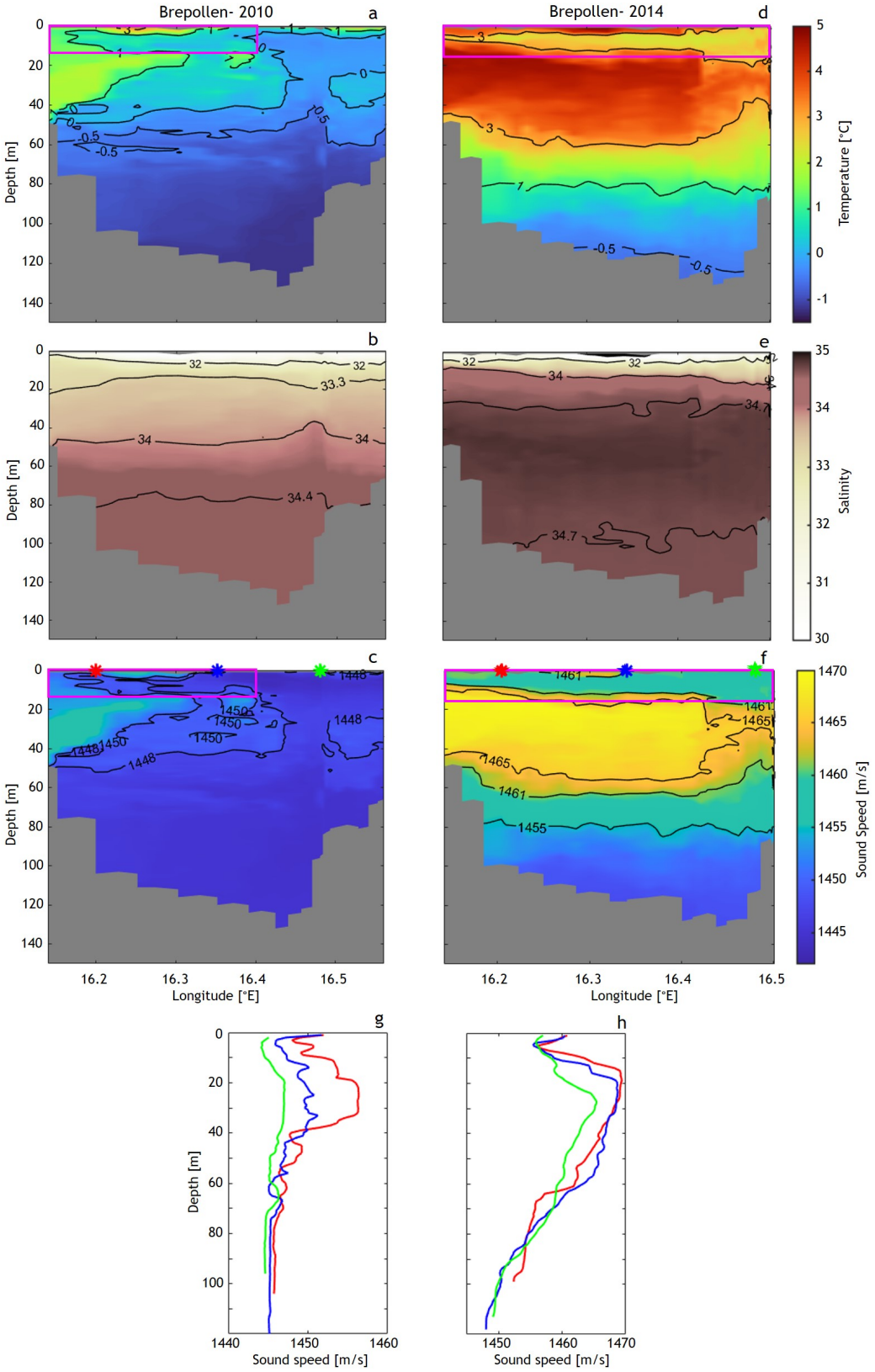

Figure 5. Distribution of water temperature (a and d), salinity (b and e) and sound speed (c and f) in Brepollen in 2010 (left panel) and 2014 (right panel). Pink rectangles indicate the surface water layers in plots a and d, and the corresponding near-surface sound channel's location in plots c and f. Sound speed profiles at three selected locations (g and h), marked by red (station near the Main Basin), dark blue (station near the middle of Brepollen) and green (station in the inner part of Brepollen) stars in the plots c and f. The colors of profiles in plots g and h correspond to the colors used to indicate the stations.

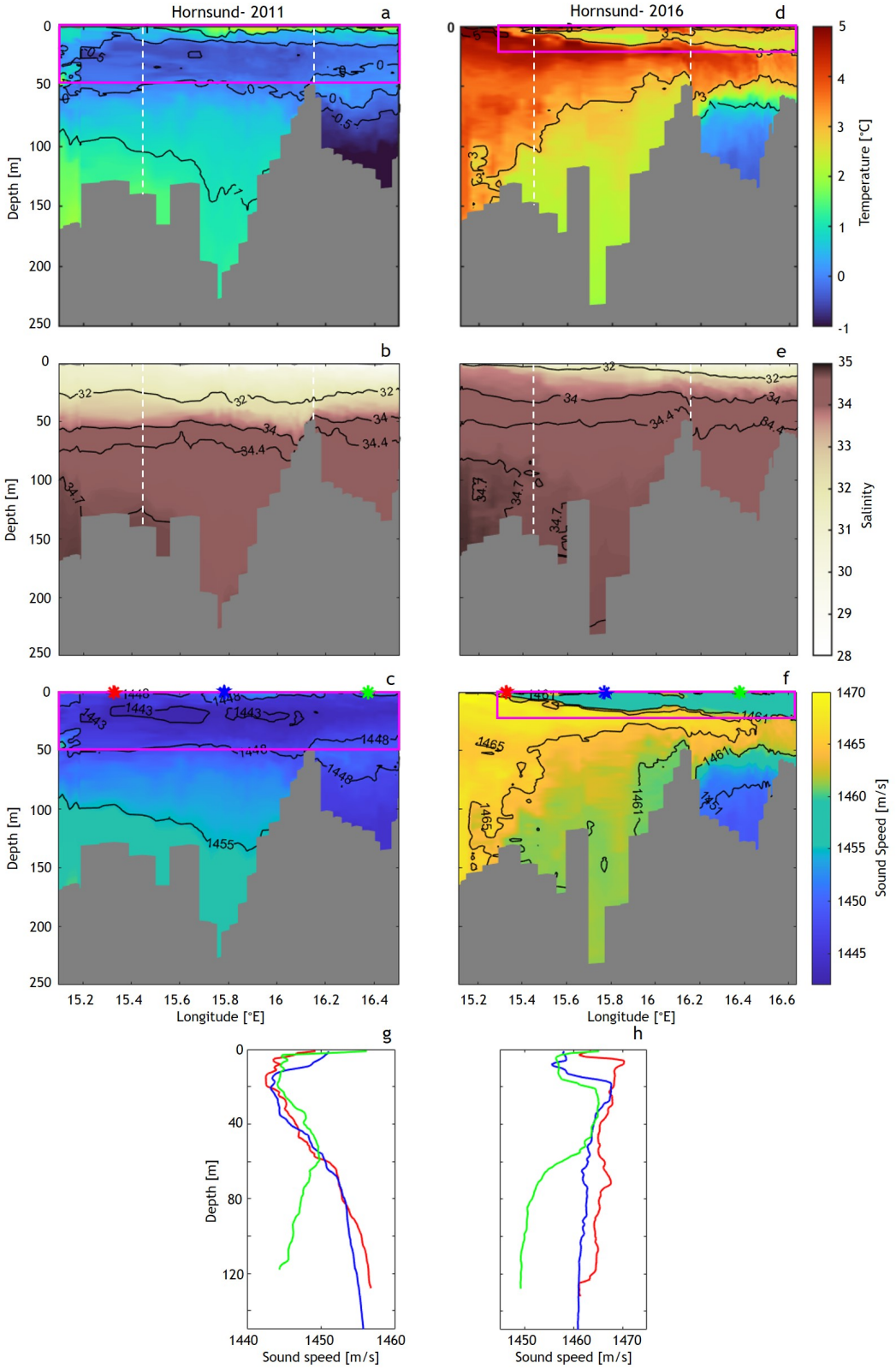

Figure 6. Distribution of water temperature (a and d), salinity (b and e) and sound speed (c and f) in the entire Hornsund in 2011 (left panel) and 2016 (right panel). The white dashed lines indicate the boundary between the Outer Part (left) and the Main Basin (middle), and Brepollen. The pink rectangles indicate the surface water layers in plots a and d, and the near-surface sound channel's location in plots c and f. Sound speed profiles at three selected locations (g and h), marked by red (station in the Outer Part), blue (station in the Main Basin) and green (station in Brepollen) stars in plots c and f. The colors of profiles in plots g and h correspond to the colors used to indicate the stations.

layer (glacially-modified water; e.g., Glowacki et al., 2016). The low salinity surface layers in Figure 5b and e in both years are likely due to the input of glacier melting water, which played an important role in shaping the local thermohaline structure and so in the formation of near-surface sound channels. Interestingly, there were notable temperature differences in the surface layer between the two years, possibly driven by variations in the local air temperature (Figure S1 in Supplementary materials). The July mean air temperature was about 2°C higher in 2014 than in 2010 (Wawrzyniak and Osuch, 2020). It should be noted that the meteorological conditions in Brepollen can be different compared to the study site, in which measurements were taken (Polish Polar Station Hornsund, located near the western part of the Main Basin). However, the warmer thin surface water layer could be the result of the increase in air temperature, which likely indicates the additional impact of the atmospheric heat flux in shaping the thermohaline structure.

Taking into account that the warmer and more saline layer below the surface layer was also responsible for the near-surface sound channel development, we considered the nature of this layer in 2010 and 2014. The influence of the Atlantic Water advection from the WSC to the fjord was significantly different in these two years (Promińska et al., 2018; Strzelewicz et al., 2022). The year 2014 was the only year when the warm Transformed Atlantic Water entered the middle layer of the entire Brepollen (Promińska et al., 2018). It was the result of enhanced advection of Atlantic Water to the fjord (Arntsen et al., 2019; Strzelewicz et al., 2022). In contrast, in 2010, the transport of warm and salty water from the Main Basin to Brepollen was limited, likely due to the significant reduction of Atlantic Water advection to the fjord (Arntsen et al., 2019; Promińska et al., 2018). Moreover, cold Arctic Water from the SPC was prominent on the shelf connected with the fjord this year (Strzelewicz et al., 2022). Stronger impact of the Atlantic Water advection towards Brepollen could be the reason for the more developed near-surface channel in 2014.

Summarising, the combined effect of melt-driven glacier meltwater influx and variable intensity of shelf-fjord water exchange (that controls the dominant water mass type on the shelf) could be important in controlling the near-surface sound channels in Brepollen.

In certain years, e.g. 2011 and 2016, near-surface sound channels extended along the entire Hornsund fjord (see Figure 3g–i). Figure 6 illustrates these two different examples of near-surface sound channels covering the entire fjord.

In 2011, a near-surface sound channel of approximately 50 m thick was developed along the entire fjord (see pink rectangle in Figure 6c and line plots in Figure 6g). The surface layer with a salinity of less than 33 and temperatures ranging from about 1–2°C at the sea surface to 0°C at 50 m depth, was observed along the entire transect of Hornsund (Figure 6a–b). Just below this layer, salinity (> 34) and temperature (> 0°C) were higher. This thermohaline structure was responsible for the creation of the near-surface sound channel. Both described layers contained Local Water.

In 2016, the near-surface sound channel extended along the fjord east to 15.30°E, and it was wider in Brepollen compared to the Outer Part (see pink rectangle in Figure 6f and line plots in Figure 6h). The surface water layer with typical temperatures of 23°C and salinity below 33, as well as warmer (> 3°C) and more saline (>34) sub-surface layer, were responsible for the presence of the channel (Figures 6d–e). The surface and sub-surface layers contained Surface Water and warm Intermediate Water, respectively.

Different mechanisms were responsible for the development of near-surface sound channels in 2011 and 2016. To support this statement, Strzelewicz et al. (2022) observed the contrasting regime of the dominant water mass type in the shelf connected to the Hornsund fjord in these two years. In 2011, the shelf connected to the fjord was occupied by Arctic Water carried by the SPC, which progressively reduced the intrusion of Atlantic Water into the fjord (please see Figures 8 and 9 in Strzelewicz et al. (2022)). Moreover, Promińska et al. (2018) also observed an immense supply of pack ice transported by the SPC entered the top layers (~ 50 m) of the fjord in the summer of this year. The melting of sea ice can cause the cold and less saline water to occupy the top layers of the water column. This was likely the main mechanism responsible for the formation of the near-surface sound channel in this year.

In 2016, a contrasting mechanism was dominant: a relatively immense supply of glacier meltwater to the fjord. As a result, the surface layer of glacially-modified water extended up to the Outer Part of the fjord, being responsible for the near-surface sound channel presence in this year (Figure 6e). The larger channel thickness in Brepollen confirmed the more pronounced influence of this mechanism on the near-surface channel formation in this region (Figure 6f and h). Furthermore, the July air temperature (6.3°C; Figure S1 in Supplementary materials) was maximum in 2016 compared to the other studied years (Wawrzyniak and Osuch, 2020), which certainly caused enhanced surface melting of glaciers located in the study site. In confirmation, Błaszczyk et al. (2023) have observed that during the period 2016–2020, the frontal ablation of glaciers was the highest in the summer of 2016.

Additionally, taking into account that the warmer and more saline layer below the surface layer also impacted the near-surface sound channel formation, it is interesting to understand the reasons behind its formation. Strzelewicz et al. (2022) observed the dominant influence of the Atlantic Water on the shelf connected with Hornsund in 2016. The fjord's sub-surface layer containing warm Intermedi-

ate Water was under the influence of the Atlantic Water from the shelf.

In summary, besides the combined effect of glacier melting and Atlantic-origin warm water input from WSC, the sea-ice advection from SPC to the fjord was also responsible for the near-surface sound channel in the Hornsund fjord. Particularly, the intensive cryogenic meltwater input can cause the formation of long near-surface sound channels, which extend along the entire fjord.

5. Major outcomes and future perspectives

We are aware of some important limitations connected with this study. Most importantly, the available CTD profiles should be considered as snapshots, because transects were taken only one day during each summer. Consequently, some of the reported changes in sound speed conditions may be caused not only by inter-annual variability but also result from seasonal fluctuations. Nevertheless, the results reported here give the first insight into the long-term evolution of sound speed conditions in Hornsund, which allows us to speculate about the future impact of climate shifts on the underwater sound transmission in this fjord and other West Spitsbergen fjords. Moreover, we acknowledged the importance of exploring the seasonality effect; however, it is not possible due to data limitations, as CTD measurements from the monitoring conducted by the Polish Polar Station Hornsund are limited to glacierised bays (Korhonen et al., 2024). Furthermore, global datasets (e.g., Copernicus, ARGO) are not available for the majority of the Hornsund area due to its small size, remote location, and no long-term moored data available on the thermohaline structure in the region.

However, the results presented here provide insight into the variability of underwater sound propagation conditions in Hornsund due to climate change. First, the presence of Atlantic Water and Transformed Atlantic Water in the Hornsund fjord prevented deep sound channel formation (see Figure 4d–f); therefore, we speculate that climate-driven warming of the fjord could eventually lead to a lack of deep sound channels. To support this hypothesis, recent studies demonstrated that the impact of Atlantic Water on the hydrography of West Spitsbergen Shelf and West Spitsbergen fjords has increased (Skogseth et al., 2020; Strzelewicz et al., 2022; Tverberg et al., 2019). Kongsfjorden and Isfjorden, two West Spitsbergen fjords located north of Hornsund, have transformed from Arctic-dominance to Atlantic-dominance over the last decade (De Rovere et al., 2022; Skogseth et al., 2020; Tverberg et al., 2019). Moreover, the presence of more Atlantic-origin water (e.g., Transformed Atlantic Water) in Hornsund has also been observed during the last decade (Jain et al., 2024; Promińska et al., 2018; Strzelewicz et al., 2022). Hornsund has preserved its Arctic dominance due to the regulating effect of cold Arctic Water from the Barents Sea, delivered by the SPC (Strzelewicz et al., 2022). Nevertheless, several studies have shown the ongoing Atlantification of the Nordic and Barents seas (Årthun et al., 2019; Lind et al., 2018; Polyakov et al., 2017; Shu et al., 2022; Wang et al., 2020); therefore, a warming trend analogous to those observed in Kongsfjorden and Isfjorden should be expected in Hornsund. The resulting lack of deep sound channels will likely promote more frequent soundwave interactions with the seabed and sea surface (higher energy loss). Consequently, the propagation range of underwater sound generated in mid-water layers may be largely reduced. However, quantitative analysis of acoustic energy loss along the Hornsund transect requires sound propagation modelling, which is beyond the scope of this study.

Second, the results demonstrate that near-surface sound channels in recent years have been more pronounced. The vertical distance between the sea surface and the shallowest local sound speed maximum increased as it was, for example, presented for Brepollen in Figure 3i (compare dark blue curve for 2010 with red and light blue curves for 2014 and 2016, respectively). Moreover, our analysis for the entire study period demonstrated that in recent years, near-surface sound channels more frequently covered the entire Hornsund fjord. These changes are almost certainly due to the accelerated glaciers retreat (Błaszczyk et al., 2013; Błaszczyk et al., 2023; van Pelt et al., 2019). The increased presence of glacially-modified water masses is favourable for the creation of near-surface sound channels (Glowacki et al., 2016; Vishnu et al., 2020). Importantly, modelling studies demonstrate that freshwater runoff in Svalbard will double by the middle of the 21st century due to the projected climate warming (Geyman et al., 2022; van Pelt et al., 2021). Moreover, it is well-known that submarine melting of glacier ice generates impulsive noise due to the explosive release of gas bubbles (e.g., Deane et al., 2014; Glowacki et al., 2018; Pettit et al., 2015; Urick, 1971). The intensity of the melt noise is highest close to the sea surface due to the largest difference between the hydrostatic pressure and gas pressure in the ice (Vishnu et al., 2023). It is important to mention that due to the sea-ice loss, shipping traffic has become more intensive, which tends to increase anthropogenic noise near the surface in the fjord (e.g., Overland et al., 2013). The combined effect of more pronounced near-surface sound channels and more intense noise – both driven by oceanic warming – will likely result in increased noise levels (sound pollution) in the top water layer. Similarly to the deep water channels, modelling studies are needed to quantify this effect.

The impact of sound pollution on marine animals' well-being is a critical concern in marine ecosystems. Many marine mammals rely on sound for their key biological functions, such as communication, feeding, mating, navigation, and prey-predator interaction, which can be particularly impacted by sound pollution (e.g., Duarte et al., 2021; Erbe et al., 2018; Erbe et al., 2019; Halliday et al., 2017; Halliday et al., 2019; Halliday et al., 2020; PAME, 2019).

Sound pollution can interfere with the ability to receive and interpret sound by marine mammals. Some marine mammals cease or interrupt communication as a result of increased levels of ship noise (Erbe et al., 2019). For example, the frequency range of underwater noise from watercraft overlaps with the vocalisation frequency band has the potential to disturb the communication of grey seals (Bagočius, 2015). Increased sound pollution can impact marine mammals by masking important sounds and even resulting in hearing loss (e.g., Erbe and Farmer, 2000; Popov et al., 2013). It can cause behavioral changes, and physiological stress (Erbe et al., 2018; Erbe et al., 2019; Erbe et al., 2016; Lyamin et al., 2011; Martin et al., 2022). For example, beluga vocalisation has decreased due to the vessel traffic (Halliday et al., 2019).

The expected ongoing warming in the Arctic may result in increased sound pollution for two reasons. The first reason is the intense growth of anthropogenic (shipping: e.g., Kystdatahuset, 2025; Rodriguez et al., 2024) and natural (glacier melting events: e.g., Błaszczyk et al., 2023) noise sources, particularly near the fjord surface, as it was mentioned above. The second reason is the impact of climate change on sound speed conditions (e.g., Affatati et al., 2022; Duda, 2017; Possenti et al., 2023). The underwater sound channels, trapping the sound and favouring the long-distance propagation of natural and anthropogenic origin noise, could impact the sound pollution level. Therefore, the changes in the underwater sound channels' occurrence and positioning under climate shift, may have far-reaching consequences on sound pollution level and so marine mammals' well-being (e.g., Duarte et al., 2021; Erbe et al., 2018; Erbe et al., 2019; PAME, 2019). This is particularly concerning in the Hornsund fjord, due to the lack of deep sound channels and the prominence of near-surface sound channels in recent years. This could lead to an increase in sound propagation range near the surface, whereas the noise fades in the mid-water layer. Therefore, sound pollution tends to increase near the surface of the fjord. Consequently, due to the dominance of near-surface sound channels and more intense surface noise sources, marine mammals that spend time near the surface (e.g. beluga or minke whales, Bengtsson et al., 2022) are likely to be more vulnerable to sound pollution. However, when those mammals dive to the mid-water layers, they are likely to be less vulnerable due to the lack of deep sound channels. The increase of natural and anthropogenic noise, together with the variability of sound channels, emphasises the importance of quantifying the effects of sound pollution on the animals residing at different depth levels in the Hornsund fjord; therefore, sound propagation modelling is crucial here.

6. Conclusion

In this study, we analysed the long-term evolution of sound speed conditions in the Hornsund fjord, Svalbard. The results showed the spatial and temporal variability of the sound speed conditions in the fjord caused by changes in the thermohaline structure, and allowed identification of major types of sound channels. Different factors governing the creation of near-surface and deep sound channels were also discussed: glacier melting, intense advection of warm Atlantic Water, intense sea-ice advection and melting, and atmospheric heat flux. Major outcomes of the study highlight the prominence of near-surface sound channels and the diminishing of deep sound channels in recent years. As a result, the sound propagation range could be larger near the surface compared to the mid-water layers in the fjord. This may have far-reaching consequences on the increased sound pollution in the top water layers of the Hornsund fjord and so on for marine mammals' well-being. Future studies should involve sound propagation modelling to quantify the impact of oceanic warming on the underwater sound transmission in Hornsund.

Author's contribution

PVMV: Conceptualization, Formal analysis, Software, Investigation, Writing – Original Draft; NG: Conceptualization, Investigation, Writing – Review & Editing, Supervision; OG: Conceptualization, Investigation, Writing – Review & Editing, Supervision

Acknowledgments

We greatly appreciate the scientific team of the Observational Oceanography Laboratory of the Physical Oceanography Department of the Institute of Oceanology of the Polish Academy of Sciences for collecting CTD data in Hornsund in the period from 2001 to 2019 and its pre-processing. This work was supported by the Institute of Oceanology of the Polish Academy of Sciences (statutory activity) and the Tricity Doctoral School, Poland. OG has been supported by the National Science Centre, Poland (grant no. 2021/43/D/ST10/00616) and the Ministry of Science and Higher Education of Poland (subsidy for the Institute of Geophysics, Polish Academy of Sciences).

Supplementary materials

Supplementary data associated with this article can be found online. Please follow this link to see the supplementary data associated with this article.

Conflict of interest

None declared.

References

Affatati, A., Scaini, C., Salon, S., 2022. *Ocean Sound Propagation in a Changing Climate: Global Sound Speed*

Changes and Identification of Acoustic Hotspots. Earth's Future 10(3). https://doi.org/10.1029/2021ef002099

Alexander, P., Duncan, A., Bose, N., Williams, G., 2016. *Modelling acoustic propagation beneath Antarctic sea ice using measured environmental parameters*. Deep Sea Res. Pt. II. 131, 84–95. http://dx.doi.org/10.1016/j.dsr2.2016.04.026

Arntsen, M., Sundfjord, A., Skogseth, R., Błaszczyk, M., Promińska, A., 2019. *Inflow of Warm Water to the Inner Hornsund Fjord, Svalbard: Exchange Mechanisms and Influence on Local Sea Ice Cover and Glacier Front Melting*. J. Geophys. Res: Oceans. 124, 1915–1931. https://doi.org/10.1029/2018jc014315

Årthun, M., Eldevik, T., Smedsrud, L.H., 2019. *The Role of Atlantic Heat Transport in Future Arctic Winter Sea Ice Loss*. J. Clim. 32, 3327–3341. https://doi.org/10.1175/jcli-d-18-0750.1

Bagočius, D., 2015. *Potential Masking of the Baltic Grey Seal Vocalisations by Underwater Shipping Noise in the Lithuanian Area of the Baltic Sea*. EREM 4(70), 66–72. https://doi.org/10.5755/j01.erem.70.4.6913

Baggeroer, A. B., Collis, J. M., 2022. *Transmission loss for the Beaufort Lens and the critica frequency for mode propagation during ICEX-18*. J. Acoust. Soc. Am. 151(4), 2760–2772. https://doi.org/10.1121/10.0010049

Ballard, M. S., 2019. *Three-dimensional acoustic propagation effects induced by the sea ice canopy*. J. Acoust. Soc. Am. 146(4), EL364–EL368. https://doi.org/10.1121/1.5129554

Ballard, M. S., Badiey, M., Sagers, J. D., Colosi, J. A., Turgut, A., Pecknold, S., Lin, Y.-T., Proshutinsky, A., Krishfield, R., Worcester, P. F., 2020. *Temporal and spatial dependence of a yearlong record of sound propagation from the Canada Basin to the Chukchi Shelf*. J. Acoust. Soc. Am. 148(3), 1663–1680. https://doi.org/10.1121/10.0001970

Bengtsson, O., Lydersen, C., Kovacs, K. M., 2022. *Cetacean spatial trends from 2005 to 2019 in Svalbard, Norway*. Polar Res. 41. http://dx.doi.org/10.33265/polar.v41.7773

Błaszczyk, M., Ignatiuk, D., Uszczyk, A., Cielecka-Nowak, K., Grabiec, M., Jania, J.A., Moskalik, M., Walczowski, W., 2019. *Freshwater input to the Arctic fjord Hornsund (Svalbard)*. Polar Res. 38. https://doi.org/10.33265/polar.v38.3506

Błaszczyk, M., Jania, J.A., Kolondra, L., 2013. *Fluctuations of tidewater glaciers in Hornsund Fjord (Southern Svalbard) since the beginning of the 20th century*. Pol. Polar Res. 34, 327–352. https://doi.org/10.2478/popore-2013-0024

Błaszczyk, M., Moskalik, M., Grabiec, M., Jania, J., Walczowski, W., Wawrzyniak, T., Strzelewicz, A., Malnes, E., Lauknes, T.R., Pfeffer, W.T., 2023. *The Response of Tidewater Glacier Termini Positions in Hornsund (Svalbard) to Climate Forcing, 1992–2020*. J. Geophys. Res. Earth Surf. 128. https://doi.org/10.1029/2022jf006911

Chauché, N., Hubbard, A., Gascard, J.C., Box, J.E., Bates, R., Koppes, M., Sole, A., Christoffersen, P., Patton, H., 2014. *Ice–ocean interaction and calving front morphology at two west Greenland tidewater outlet glaciers*. Cryosphere 8, 1457–1468. https://doi.org/10.5194/tc-8-1457-2014

Chen, C.-T., Millero, F.J., 1977. *Sound speed in seawater at high pressures*. J. Acoust. Soc. Am. 62, 1129–1135. https://doi.org/10.1121/1.381646

Chitre, M., Shahabudeen, S., Stojanovic, M., 2008. *Underwater acoustic communications and networking: Recent advances and future challenges*. Mar. Technol. Soc. J. 42, 103–116. https://doi.org/10.4031/002533208786861263

Cook, A.J., Copland, L., Noël, B.P., Stokes, C.R., Bentley, M.J., Sharp, M.J., Bingham, R.G., van den Broeke, M.R., 2019. *Atmospheric forcing of rapid marine-terminating glacier retreat in the Canadian Arctic Archipelago*. Sci. Adv. 5. https://doi.org/10.1126/sciadv.aau8507

Dahlke, S., Hughes, N.E., Wagner, P.M., Gerland, S., Wawrzyniak, T., Ivanov, B., Maturilli, M., 2020. *The observed recent surface air temperature development across Svalbard and concurring footprints in local sea ice cover*. Int. J. Climatol. 40, 5246–5265. https://doi.org/10.1002/joc.6517

De Rovere, F., Langone, L., Schroeder, K., Miserocchi, S., Giglio, F., Aliani, S., Chiggiato, J., 2022. *Water Masses Variability in Inner Kongsfjorden (Svalbard) During 2010–2020*. Front. Mar. Sci. 9. https://doi.org/10.3389/fmars.2022.741075

Deane, G.B., Glowacki, O., Stokes, D., Pettit. E., 2019. *The Underwater Sounds of Glaciers*. Acoust. Today. 15, 12. https://doi.org/10.1121/at.2019.15.4.12

Deane, G.B., Glowacki, O., Tegowski, J., Moskalik, M., Blondel, P., 2014. *Directionality of the ambient noise field in an Arctic, glacial bay*. J. Acoust. Soc. Am. 136, EL350-6. https://doi.org/10.1121/1.4897354

Diachok, O. I., 1976. *Effects of sea-ice ridges on sound propagation in the Arctic Ocean*. J. Acoust. Soc. Am. 59(5), 1110–1120. https://doi.org/10.1121/1.380965

Duarte, C.M., Chapuis, L., Collin, S.P., Costa, D.P., Devassy, R.P., Eguiluz, V.M., Erbe, C., Gordon, T.A.C., Halpern, B.S., Harding, H.R., Havlik, M.N., Meekan, M., Merchant, N.D., Miksis-Olds, J.L., Parsons, M., Predragovic, M., Radford, A.N., Radford, C.A., Simpson, S.D., Slabbekoorn, H., Staaterman, E., Van Opzeeland, I.C., Winderen, J., Zhang, X., Juanes, F., 2021. *The soundscape of the Anthropocene ocean*. Science 371. https://doi.org/10.1126/science.aba4658

Duda, T. F., 2017. *Acoustic signal and noise changes in the Beaufort Sea Pacific Water duct under anticipated future acidification of Arctic Ocean waters*. J. Acoust. Soc. Am. 142(4), 1926–1933. https://doi.org/10.1121/1.5006184

Duda, T. F., Zhang, W. G., Lin, Y. T., 2021. *Effects of Pacific Summer Water layer variations and ice cover on Beaufort Sea underwater sound ducting*. J. Acoust. Soc. Am. 149(4), 2117–2136. https://doi.org/10.1121/10.0003929

Erbe, C., Dunlop, R., Dolman, S., 2018. *Effects of Noise on Marine Mammals*. [in:] Slabbekoorn, H., Dooling, R.J., Popper, A.N., Fay, R.R. (Eds.), *Effects of Anthropogenic Noise on Animals*. Springer Handbook of Auditory Research, 277–309. https://doi.org/10.1007/978-1-4939-8574-6

Erbe, C., Farmer, D. M., 2000. *Zones of impact around icebreakers affecting beluga whales in the Beaufort Sea*. J. Acoust. Soc. Am. 108(3), 1332–1340. https://doi.org/10.1121/1.1288938

Erbe, C., Marley, S.A., Schoeman, R.P., Smith, J.N., Trigg, L.E., Embling, C.B., 2019. *The Effects of Ship Noise on Marine Mammals — A Review*. Front. Mar. Sci. 6. https://doi.org/10.3389/fmars.2019.00606

Erbe, C., Reichmuth, C., Cunningham, K., Lucke, K., Dooling, R., 2016. *Communication masking in marine mammals: A review and research strategy*. Mar. Pollut. Bull. 103, 15–38. https://doi.org/10.1016/j.marpolbul.2015.12.007

Geyman, E.C., W, J.J.v.P., Maloof, A.C., Aas, H.F., Kohler, J., 2022. *Historical glacier change on Svalbard predicts doubling of mass loss by 2100*. Nature. 601, 374–379. https://doi.org/10.1038/s41586-021-04314-4

Gjelten, H.M., Nordli, Ø., Isaksen, K., Førland, E.J., Sviashchennikov, P.N., Wyszynski, P., Prokhorova, U.V., Przybylak, R., Ivanov, B.V., Urazgildeeva, A.V., 2016. *Air temperature variations and gradients along the coast and fjords of western Spitsbergen*. Polar Res. 35, 29878. https://doi.org/10.3402/polar.v35.29878

Glowacki, O., 2020. *Underwater noise from glacier calving: Field observations and pool experiment*. J. Acoust. Soc. Am. 148, EL1–EL7. https://doi.org/10.1121/10.0001494

Glowacki, O., Deane, G.B., Moskalik, M., 2018. *The Intensity, Directionality, and Statistics of Underwater Noise From Melting Icebergs*. Geophys. Res. Lett. 45, 4105–4113. https://doi.org/10.1029/2018gl077632

Glowacki, O., Deane, G.B., Moskalik, M., Blondel, P., Tegowski, J., Blaszczyk, M., 2015. *Underwater acoustic signatures of glacier calving*. Geophys. Res. Lett. 42, 804–812. https://doi.org/10.1002/2014gl062859

Glowacki, O., Moskalik, M., Deane, G.B., 2016. *The impact of glacier meltwater on the underwater noise field in a glacial bay*. J. Geophys. Res: Oceans. 121, 8455–8470. https://doi.org/10.1002/2016jc012355

Glowacki, O., Moskalik, M., Prominska, A., 2013. *Simulation of the sound propagation in an Arctic fjord: general patterns and variability*. poster presented at Arctic Science Summit Week, Committee on Polar Research of the Polish Academy of Sciences, Cracow, Poland.

Halliday, W. D., Insley, S. J., Hilliard, R. C., de Jong, T. Pine, M. K., 2017. *Potential impacts of shipping noise on marine mammals in the western Canadian Arctic*. Mar. Pollut. Bull. 123(1–2), 73–82. http://dx.doi.org/10.1016/j.marpolbul.2017.09.027

Halliday, W. D., Pine, M. K. Insley, S. J., 2020. *Underwater noise and Arctic marine mammals: Review and policy recommendations*. Environ. Rev. 28(4), 438–448. https://doi.org/10.1139/er-2019-003

Halliday, W. D., Scharffenberg, K., MacPhee, S., Hilliard, R. C., Mouy, X., Whalen, D., Loseto, L. L. Insley, S. J., 2019. *Beluga Vocalizations Decrease in Response to Vessel Traffic in the Mackenzie River Estuary*. Arctic. 72(4), 337–346. https://doi.org/10.14430/arctic69294

Holmes, F.A., Kirchner, N., Kuttenkeuler, J., Krutzfeldt, J., Noormets, R., 2019. *Relating ocean temperatures to frontal ablation rates at Svalbard tidewater glaciers: Insights from glacier proximal datasets*. Sci. Rep. 9, 9442. https://doi.org/10.1038/s41598-019-45077-3

Hopkins, T.S., 1991. *The GIN Sea—A synthesis of its physical oceanography and literature review 1972–1985*. Earth-Sci. Rev. 30, 175–318. https://doi.org/10.1016/0012-8252(91)90001-V

IPCC 2021. *Climate change 2021: The physical science basis*. Contribution of working group I to the sixth assessment report of the intergovernmental panel on climate change.

Jain, V., Korhonen, M., Głowacki, O. Moskalik, M., 2024. *Hydrography of the Inner Basins in Hornsund (Svalbard): Heat Advection Near Tidewater Glaciers*. J. Geophys. Res.: Oceans, 129(11). https://doi.org/10.1029/2024JC021273

Jakacki, J., Przyborska, A., Kosecki, S., Sundfjord, A., Albretsen, J., 2017. *Modelling of the Svalbard fjord Hornsund*. Oceanologia 59(4), 473–495. https://doi.org/10.1016/j.oceano.2017.04.004

Jensen, F.B., Kuperman, W.A., Porter, M.B., Schmidt, H., Tolstoy, A., 2011. *Computational ocean acoustics*. 2nd edn., Springer, New York.

Korhonen, M., Moskalik, M., Głowacki, O., Jain, V., 2024. *Oceanographic monitoring in Hornsund fjord, Svalbard*. Earth Syst. Sci. Data. 16(10), 4511–4527. https://doi.org/10.5194/essd-16-4511-2024

Kucukosmanoglu, M., Colosi, J. A., Worcester, P. F., Dzieciuch, M. A., Sagen, H., Duda, T. F., Zhang, W. G., Miller, C. W., Richards, E. L., 2023. *Observations of the space/time scales of Beaufort sea acoustic duct variability and their impact on transmission loss via the mode interaction*

parameter. J. Acoust. Soc. Am. 153(5), 2659–2676. https://doi.org/10.1121/10.0019335

Kutschale, H., 1969. *Arctic hydroacoustics*. Arctic. 22, 169–364. https://doi.org/10.14430/arctic3218

Kystdatahuset, 2025. *Tall og statistikk-Trafikk i område*. https://kystdatahuset.no/tallogstatistikk/trafikkiomrade (Accessed 01.07.2025).

Lind, S., Ingvaldsen, R.B., Furevik, T., 2018. *Arctic warming hotspot in the northern Barents Sea linked to declining sea-ice import*. Nat. Clim. Change. 8, 634–639. https://doi.org/10.1038/s41558-018-0205-y

Luckman, A., Benn, D.I., Cottier, F., Bevan, S., Nilsen, F., Inall, M., 2015. *Calving rates at tidewater glaciers vary strongly with ocean temperature*. Nat. Commun. 6, 8566. https://doi.org/10.1038/ncomms9566

Lyamin, O. I., Korneva, S. M., Rozhnov, V. V., Mukhametov, L. M., 2011. *Cardiorespiratory changes in beluga in response to acoustic noise*. Dokl. Biol. Sci. 440(5), 275–278. https://doi.org/10.1134/S0012496611050218

Lynch, J., Gawarkiewicz, G., Lin, Y.-T., Duda, T., Newhall, A., 2018. *Impacts of Ocean Warming on Acoustic Propagation Over Continental Shelf and Slope Regions*. Oceanography 31(2), 174–181. https://doi.org/10.5670/oceanog.2018.219

Marsz, A.A., Styszyńska, A., 2013. *Climate and climate change at Hornsund, Svalbard*. Gdynia Marit. Univ., Gdynia, ISBN: 978-83-7421-191-8.

Martin, M. J., Halliday, W. D., Storrie, L., Citta, J. J., Dawson, J., Hussey, N. E., Juanes, F., Loseto, L. L., MacPhee, S. A., Moore, L., Nicoll, A., O'Corry-Crowe, G., Insley, S. J., 2022. *Exposure and behavioral responses of tagged beluga whales (Delphinapterus leucas) to ships in the Pacific Arctic*. Mar. Mamm. Sci. 39(2), 387–421. https://doi.org/10.1111/mms.12978

Matsumoto, H., Bohnenstiehl, D.R., Tournadre, J., Dziak, R.P., Haxel, J.H., Lau, T.K.A., Fowler, M., Salo, S.A., 2014. *Antarctic icebergs: A significant natural ocean sound source in the Southern Hemisphere*. Geochem. Geophys. 15, 3448–3458. https://doi.org/10.1002/2014gc005454

McCammon, D. F., McDaniel, S. T., 1985. *The influence of the physical properties of ice on reflectivity*. J. Acoust. Soc. Am. 77(2), 499–507. https://doi.org/10.1121/1.391869

Medwin, H., Clay, C.S., 1998. *Fundamentals of acoustical oceanography*. Acad. Press, New York.

Meyer, A., Eliseev, D., Heinen, D., Linder, P., Scholz, F., Weinstock, L. S., Wiebusch, C., Zierke, S., 2019. *Attenuation of sound in glacier ice from 2 to 35 kHz*. The Cryosphere. 13(4), 1381–1394. https://doi.org/10.5194/tc-13-1381-2019

Moskalik, M., Grabowiecki, P., Tęgowski, J., Żulichowska, M., 2013. *Bathymetry and geographical regionalization of Brepollen (Hornsund, Spitsbergen) based on bathymetric profiles interpolations*. Pol. Polar Res. 34, 1–22. https://doi.org/10.2478/popore–2013–0001

Munk, W., Worcester, P., Wunsch, C., 1995. *Ocean acoustic tomography*. Cambridge Univ. Press, Cambridge, England.

Nilsen, F., Cottier, F., Skogseth, R., Mattsson, S., 2008. *Fjord–shelf exchanges controlled by ice and brine production: The interannual variation of Atlantic Water in Isfjorden, Svalbard*. Cont. Shelf Res. 28, 1838–1853. https://doi.org/10.1016/j.csr.2008.04.015

Nilsen, F., Skogseth, R., Vaardal-Lunde, J., Inall, M., 2016. *A Simple Shelf Circulation Model: Intrusion of Atlantic Water on the West Spitsbergen Shelf*. J. Phys. Oceanogr. 46, 1209–1230. https://doi.org/10.1175/jpo-d-15-0058.1

Overland, J.E., Wang, M., Walsh, J.E., Stroeve, J.C., 2013. *Future Arctic climate changes: Adaptation and mitigation time scales*. Earth's Future. 2, 68–74. https://doi.org/10.1002/2013ef000162

PAME 2019. *Underwater noise in the Arctic: A state of knowledge report*. Protection of the Arctic Marine Environment (PAME) International Secretariat.

PAME, 2025. *PAME*, Arctic Shipping Status Rep.no 1. https://hdl.handle.net/11374/2733.3

Pettit, E.C., Lee, K.M., Brann, J.P., Nystuen, J.A., Wilson, P.S., O'Neel, S., 2015. *Unusually loud ambient noise in tidewater glacier fjords: A signal of ice melt*. Geophys. Res. Lett. 42, 2309–2316. https://doi.org/10.1002/2014GL062950

Podolskiy, E.A., Murai, Y., Kanna, N., Sugiyama, S., 2022. *Glacial earthquake-generating iceberg calving in a narwhal summering ground: The loudest underwater sound in the Arctic*? J. Acoust. Soc. Am. 151(1), 6–16. https://doi.org/10.1121/10.0009166

Polyakov, I.V., Pnyushkov, A.V., Alkire, M.B., Ashik, I.M., Baumann, T.M., Carmack, E.C., Goszczko, I., Guthrie, J., Ivanov, V.V., Kanzow, T., 2017. *Greater role for Atlantic inflows on sea-ice loss in the Eurasian Basin of the Arctic Ocean*. Science. 356, 285–291. https://doi.org/10.1126/science.aai8204

Popov, V. V., Supin, A. Y., Rozhnov, V. V., Nechaev, D. I., Sysuyeva, E. V., Klishin, V. O., Pletenko, M. G., Tarakanov, M. B., 2013. *Hearing threshold shifts and recovery after noise exposure in beluga whales, Delphinapterus leucas*. J. Exp. Biol. 216(9), 1587–1596. https://doi.org/1587-1596,10.1242/jeb.078345

Possenti, L., Reichart, G. J., de Nooijer, L., Lam, F. P., de Jong, C., Colin, M., Binnerts, B., Boot, A., von der Heydt, A., 2023. *Predicting the contribution of climate change on North Atlantic underwater sound propagation*. PeerJ, 11 pp . https://doi.org/10.7717/peerj.16208

Promińska, A., Cisek, M., Walczowski, W., 2017. *Kongsfjorden and Hornsund hydrography – comparative study based on a multiyear survey in fjords of west Spitsbergen*. Oceanologia 59(4), 397–412. https://doi.org/10.1016/j.oceano.2017.07.003

Promińska, A., Falck, E., Walczowski, W., 2018. *Interannual variability in hydrography and water mass distribution in Hornsund, an Arctic fjord in Svalbard*. Polar Res. 37, 1495546. https://doi.org/10.1080/17518369.2018.1495546

Rodriguez, J. P., Klemm, K., Duarte, C. M., Eguiluz, V. M., 2024. *Shipping traffic through the Arctic Ocean: Spatial distribution, seasonal variation, and its dependence on the sea ice extent*. iScience 27(7), 110236. https://doi.org/10.1016/j.isci.2024.110236

Shu, Q., Wang, Q., Årthun, M., Wang, S., Song, Z., Zhang, M., Qiao, F., 2022. *Arctic Ocean Amplification in a warming climate in CMIP6 models*. Sci. Adv. 8(30). https://doi.org/10.1126/sciadv.abn9755

Skogseth, R., Olivier, L.L.A., Nilsen, F., Falck, E., Fraser, N., Tverberg, V., Ledang, A.B., Vader, A., Jonassen, M.O., Søreide, J., Cottier, F., Berge, J., Ivanov, B.V., Falk-Petersen, S., 2020. *Variability and decadal trends in the Isfjorden (Svalbard) ocean climate and circulation – An indicator for climate change in the European Arctic*. Prog. Oceanogr. 187. https://doi.org/10.1016/j.pocean.2020.102394

Slater, D.A., Straneo, F., 2022. *Submarine melting of glaciers in Greenland amplified by atmospheric warming*. Nat. Geosci. 15, 794–799. https://doi.org/10.1038/s41561-022-01035-9

Storheim, E., Sagen, H., Dzieciuch, M. A., Worcester, P. F., 2022. *Modelling of sound propagation across the Arctic Ocean using oceanographic fields and oceanographic data*. J. Acoust. Soc. Am. 152(4). https://doi.org/10.1121/10.0010047

Straneo, F., Curry, R.G., Sutherland, D.A., Hamilton, G.S., Cenedese, C., Våge, K., Stearns, L.A., 2011. *Impact of fjord dynamics and glacial runoff on the circulation near Helheim Glacier*. Nat. Geosci. 4, 322–327. https://doi.org/10.1038/ngeo1109

Strzelewicz, A., Przyborska, A., Walczowski, W., 2022. *Increased presence of Atlantic Water on the shelf southwest of Spitsbergen with implications for the Arctic fjord Hornsund*. Prog. Oceanogr. 200, 102714. https://doi.org/10.1016/j.pocean.2021.102714

Tverberg, V., Skogseth, R., Cottier, F., Sundfjord, A., Walczowski, W., Inall, M.E., Falck, E., Pavlova, O., Nilsen, F., 2019. *The Kongsfjorden transect: seasonal and interannual variability in hydrography*. [in:] Haakon, H., Christian, W. (Eds.), *The Ecosystem of Kongsfjorden*, Svalbard. Springer, Cham. 2, 49–104. https://doi.org/10.1007/978-3-319-46425-1_3

Urick, R.J., 1971. *The noise of melting icebergs*. J. Acoust. Soc. Am. 50, 337–341. https://doi.org/10.1121/1.1912637

Urick, R.J., 1979. *Sound propagation in the sea*. Defence Adv. Res. Project Agency, Washington, D. C.

van Pelt, W., Pohjola, V., Pettersson, R., Marchenko, S., Kohler, J., Luks, B., Hagen, J.O., Schuler, T.V., Dunse, T., Noël, B., Reijmer, C., 2019. *A long-term dataset of climatic mass balance, snow conditions, and runoff in Svalbard (1957–2018)*. Cryosphere. 13, 2259-02280. https://doi.org/10.5194/tc-13-2259-2019

van Pelt, W.J.J., Schuler, T.V., Pohjola, V.A., Pettersson, R., 2021. *Accelerating future mass loss of Svalbard glaciers from a multi-model ensemble*. J. Glaciol. 67, 485–0499. https://doi.org/10.1017/jog.2021.2

Vishnu, H., Deane, G.B., Chitre, M., Glowacki, O., Stokes, D., Moskalik, M., 2020. *Vertical directionality and spatial coherence of the sound field in glacial bays in Hornsund Fjord*. J. Acoust. Soc. Am. 148, 3849–3862. https://doi.org/10.1121/10.0002868

Vishnu, H., Deane, G.B., Glowacki, O., Chitre, M., Johnson, H., Moskalik, M., Stokes, D., 2023. *Depth-dependence of the underwater noise emission from melting glacier ice*. JASA Express Lett. 3, 020801-1-020801-7. https://doi.org/10.1121/10.0017348

Walczowski, W., Piechura, J., 2011. *Influence of the West Spitsbergen Current on the local climate*. Int. J. Climatol. 31, 1088–1093. https://doi.org/10.1002/joc.2338

Wang, Q., Wekerle, C., Wang, X., Danilov, S., Koldunov, N., Sein, D., Sidorenko, D., von Appen, W.J., Jung, T., 2020. *Intensification of the Atlantic Water Supply to the Arctic Ocean Through the Fram Strait Induced by Arctic Sea Ice Decline*. Geophys. Res. Lett. 47(3), e2019GL086682. https://doi.org/10.1029/2019gl086682

Wawrzyniak, T., Osuch, M., 2020. *A 40-year High Arctic climatological dataset of the Polish Polar Station Hornsund (SW Spitsbergen, Svalbard)*. Earth Syst. Sci. Data. 12, 805–815. https://doi.org/10.5194/essd-12-805-2020

Worcester, P. F., Badiey, M., Sagen, H., 2022. *Introduction to the special issue on ocean acoustics in the changing Arctic*. J. Acoust. Soc. Am. 151(4), 2787–2790. https://doi.org/10.1121/10.0010308

Worcester, P. F., Dzieciuch, M. A., Sagen, H., 2020. *Ocean Acoustics in the Rapidly Changing Arctic*. Acoust. Today. 16(1), 55–64. https://doi.org/10.1121/AT.2020.16.1.55

Zeh, M. C., Ballard, M. S., Glowacki, O., Deane, G. B., Wilson, P. S., 2022. *Model-data comparison of sound propagation in a glacierised fjord with a simulated brash ice surface*. J. Acoust. Soc. Am. 151(4), 2367–2377. https://doi.org/10.1121/10.0010046